Molecular Vision 2017; 23:933-943 <http://www.molvis.org/molvis/v23/933>
Received 10 July 2017 | Accepted 11 December 2017 | Published 13 December 2017

Substance P prevents development of proliferative vitreoretinopathy in mice by modulating TNF-α

Kyungsang Yoo,[1] Bo Kwon Son,[2] Suna Kim,[1] Youngsook Son,[1] Seung-Young Yu,[2] Hyun Sook Hong[3]

(The first two authors contributed equally to this work)

[1]Graduate School of Biotechnology, College of Life Sciences, Kyung Hee University, Seochun-dong, Kiheung-ku, Yong In, Korea; [2]Department of Ophthalmology, Kyung Hee University Hospital, Kyung Hee University, Kyungheedae-ro, Dongdaemun-gu, Seoul, Republic of Korea; [3]College of Medicine, Graduate School, Kyung Hee University, Kyungheedae-ro, Dongdaemun-gu, Seoul, Republic of Korea

Purpose: Proliferative vitreoretinopathy (PVR) is an inflammatory fibrotic disease resulting from the inflammatory milieu after retinal detachment, which can prevent retinal healing. This study aimed to elucidate the effect of substance P (SP) on retinal degeneration caused by retinal detachment in vivo and to examine the role of SP in the tumor necrosis factor-alpha (TNF-α)-induced epithelial-mesenchymal transition (EMT) of human RPE cells in vitro.
Methods: PVR-like retinal damage was induced by intravitreally injecting dispase into mice, and SP was systemically injected twice a week for 3 weeks. Histological analysis and cytokine profile with enzyme-linked immunosorbent assay (ELISA) were performed. The direct effect of SP on induction of EMT in vitro was studied by adding SP to TNF-α-treated ARPE-19 cells and then evaluating the change in the characteristics of the epithelial and mesenchymal cells.
Results: Dispase injection led to a PVR-like retinal condition, demonstrating an inflammatory response with disruption of RPE interaction within 1 week and severe destruction with enfolding within 3 weeks after the dispase injection. The inflammatory environment promoted apoptosis and migration of fibroblast-like cells in the retinal layer, which can cause fibrotic disease, such as PVR. However, SP treatment suppressed early inflammatory responses by reducing TNF-α and elevating interleukin-10 (IL-10), with cell death and the appearance of fibroblastic cells inhibited and the progression of retinal degeneration obviously delayed. Moreover, SP ameliorated TNF-α-induced EMT of the RPE and directly prevented fibrotic change in the RPE.
Conclusions: This study revealed that SP can block apoptosis and EMT due to retinal inflammation and inhibit the development of PVR. This effect most likely occurred by modulating the secretion and action of TNF-α..

Proliferative vitreoretinopathy (PVR) is a vision-threatening disease and the most common cause of failed repair of rhegmatogenous retinal detachment (RRD). Retinal detachment causes damage in the blood–retinal barrier (BRB), which permits infiltration of proinflammatory cytokines and various cells, including macrophages, RPE cells, glial cells, and fibroblasts into the vitreous and subretinal space. In this space, the cells proliferate, survive, and produce extracellular matrix (ECM) as collagen, leading to the formation of a contractible membrane on the surface of the detached retina and to retinal degeneration and vision loss [1-6].

RPE is considered a key factor in PVR development because epithelial-to-mesenchymal transition (EMT) of RPE is a critical contributor to fibrosis development. Several studies have revealed that hypoxia, inflammation, and mechanical damage cause RPE transformation into fibroblast-like cells via a process known as EMT, which leads to fibrous tissue formation in PVR [6,7]. Under an inflammatory environment, cytokines, including platelet-derived growth factor, fibroblast growth factor, and transforming growth factor b1 (TGF-β1), and transcription factors, such as Snail, are involved in the EMT of the RPE. Notably, as TGF-β1 expressed in pathological vitreous has been related to the induction of apoptosis in various cell types, as well as EMT [8-13], TGF-β1 has been considered a major factor in EMT modulation during the development of PVR [14-16]. Recently, tumor necrosis factor-alpha (TNF-α), one of the most prominent inflammatory cytokines, has emerged as a promoter of PVR. It was found that TNF-α has a causative role in PVR by acting on the RPE and inducing change in cellular morphology into fibroblastic cells. Moreover, the combination of TNF-α and TGF-β1 has strong synergistic effects to induce EMT-associated fibrotic focus formation. TNF-α was involved in the activation of TGF-β1 signaling that leads to induction of the mesenchymal phenotype in RPE [17]. As another cytokine associated with the control of EMT, interleukin-10 (IL-10) has been extensively investigated.

Correspondence to: Hyun Sook Hong, College of Medicine/ East-West Medical Research Institute, Kyung Hee University, 1 Hoegidong Dongdaemun-gu, Seoul 130-702, South Korea Phone: +82-2-958-1828; FAX: 82-31-201-3829; email: hshong@khu.ac.kr

IL-10 was found to control TGF-β1 by acting as a potent antagonist of TGF-β1 production and blocking TGF-β1 signaling [18]. Carrington et al. revealed that IL-10 can inhibit RPE-mediated retinal contraction [19]. Based on previous data, it was surmised that the control of soluble mediators, such as cytokines and growth factors, is able to alleviate the EMT of the RPE and block the development of PVR.

Substance P (SP), an endogenous neuropeptide that signals via the neurokinin-1 receptor (NK-1R), is expressed on non-neuronal cells, as well as on neuronal cells. SP modulates neuroimmune responses in the bone marrow [20] and reepithelialization in the cornea [21]. Hong et al. identified a novel role of SP as an injury-inducible messenger that mobilizes endogenous stem cells from the bone marrow to the circulation to accelerate tissue repair [22-26]. SP also exerts anti-inflammatory effects on acute inflammatory diseases and promotes wound healing [25-28]. When peripheral blood mononuclear cells (PBMCs) were treated with SP, T_{reg} or M2 macrophages were enriched in combination with increases in IL-10 and reduced TNF-α levels [27]. SP showed an inhibitory effect on TNF-α-induced apoptosis, mediated via NK-1R [29]. Moreover, independent of the effect of SP on stem cell mobilization and inflammatory responses, SP was able to increase the expression of intercellular junctional molecules, including ZO-1, to maintain a tight junction and reinforce the barrier function of epithelial cells [30]. Taking these functions of SP into account, we postulated that SP is able to inhibit the EMT of the RPE and the progression of PVR, possibly by modulating the cytokine profile or upregulating tight junction molecules in early inflammatory environments after retinal injury.

To assess the effects of SP on PVR-like damage, we used a dispase-induced retinal damage model [31-34]. The efficacy of SP was explored by analyzing the retinal structure, cytokine profile, apoptosis, and infiltration of fibroblastic cells. To examine the effect of SP on the EMT of the RPE, an in vitro model of EMT-associated fibrosis was established by treating ARPE-19 with TNF-α, and changes in cell junction molecules, actin structure, and the characteristics of mesenchymal and epithelial cells were investigated.

METHODS

Animals: Five-week-old male C57BL/6 mice were purchased from DBL (Daehan Bio Link, Seoul, South Korea). All experiments adhered to the ARVO Statement for the Use of Animals in Ophthalmic and Vision Research and were approved by the Institutional Animal Care and Use Committee of Kyung Hee University (KHUASP (SU)-11-14).

Induction of PVR: Animals were anesthetized with an intraperitoneal injection of ketamine (100 mg/kg, . Yuhan. Co., Seoul, Korea) and Rompun (1.2 mg/kg, Bayer Healthcare, Berlin, Germany). Pupils were dilated with 2.5% phenylephrine HCl (Mydfrin, Alcon, Fort Worth, TX). Intravitreal injection of dispase (0.05 U/eye, volume 2 µl, Sigma-Aldrich, St. Louis, MO) was performed in the dorsonasal quadrant 1.5 mm from the corneal limbus using a 30-gauge needle mounted on a 10 µl Hamilton syringe. After intravitreal injection of dispase, the animals were divided into two treatment groups. Mice with severe subretinal hemorrhage were excluded from analysis. At 1 and 3 weeks post-dispase injection the mice is anesthetized by injecting ketamin and rumpun intraperitoneally for further analysis.

Administration of substance P: Substance P (5 nmole/kg, volume 100 µl, Sigma-Aldrich) was intravenously administered immediately and 24 h after dispase injection. The SP injection was repeated twice weekly for 3 weeks. Saline served as the vehicle.

Histological analysis: Whole eyes were fixed in 3.7% paraformaldehyde for 1 day and then processed with a TP1020 tissue processor (Leica Biosystems, Wetzlar, Germany) for the paraffin block. Immunohistochemical staining was performed following the VECTASTAIN ABC Kit protocol (Vector Laboratories, Burlingame, CA). In brief, samples were treated with 0.5% H_2O_2 to block activity of endogenous hydrogen peroxidase and permeabilized with 0.3% Triton X-100. After blocking for nonspecific binding in 1% normal horse serum for 1 h at room temperature (RT), primary antibodies against cleaved caspase 3 and α-SMA (Abcam, Cambridge, MA) were treated. After washing in PBS (137 mM NaCl; 2.7 mM KCl; 4.3 mM Na_2HPO_4; 1.47 mM KH_2PO_4; pH 7.4), the samples were incubated with a biotin-conjugated secondary antibody for 1 h at RT. After washing in PBS, substrate solution was added for 1 h and maintained at RT. To visualize the reactive area in the tissue, the samples were treated with NovaRED™ (Vector Laboratories), counterstained for nuclei with hematoxylin (Vector Laboratories) for 1 min, and then mounted.

Quantification of the injured retina: Sectioned paraffin samples were stained with hematoxylin and eosin (Sigma-Aldrich). Samples were observed under a Nuance Multiplex Biomarker Imaging System (Cambridge Research Instrumentation, Moburn, MA). The cell numbers in the outer nuclear layer (ONL) and the inner nuclear layer (INL) were measured in six adjacent fields on temporal slides.

Measurement of cytokines: At 1 and 3 weeks post-injection of dispase, whole blood was collected and the serum separated. The TNF-α and IL-10 concentrations in serum

were measured with enzyme-linked immunosorbent assay (ELISA; R&D Systems, Minneapolis, MN) according to the manufacturer's instructions. Primary antibody-coated wells received 50 µl of the standard, control, or sample and were incubated for 2 h at RT. Next, 50 µl of the enzyme-conjugated secondary antibody solution was treated in each well for 2 h. After washing with buffer four times, the wells were then incubated with 100 µl of substrate solution in darkness. Once the solution color changed to blue, the reaction was stopped, and the optical density was measured with the wavelength correction set to 450 nm using the EMax Endpoint ELISA microplate reader (Molecular Devices, Sunnyvale, CA). The concentrations of TNF-α and IL-10 were calculated using corresponding standard curves.

In vitro EMT: ARPE-19 cells, a human RPE cell line, were grown in DMEM-F12 supplemented with 10% fetal bovine serum (FBS). After being deprived of serum for 24 h, the ARPE-19 cells were treated with TNF-α (10 ng/ml) with SP (final concentration, 100 nM) for 24 h followed by SP treatment (100 nM). At 48 h post TNF-α treatment, the cells were fixed or lysed for analysis.

STR analysis: Short tandem repeat (STR) loci were analyzed in Cosmo genetech (Seoul, Korea) using GeneMapper® ID-X v1.2 software (Applied Biosystems, Suzhou, China). Appropriate positive and negative controls were run and confirmed for each sample submitted. The STR analyses are presented in Appendix 1.

Immunofluorescence staining: Cells were fixed in 3.7% paraformaldehyde for 20 min at RT and permeabilized with 0.3% Triton X-100. After blocking with 20% goat serum (Vector Laboratories), the cells were incubated with α-SMA (Abcam) for 2 h in RT. After washing in PBS, fluorescein isothiocyanate (FITC)-anti-rabbit immunoglobulin G (IgG; Vector Laboratories) was added for 1 h. F-actin was stained with rhodamine-phalloidin (Thermo Scientific, Rockford, IL) diluted 1:100 in PBS for 15 min. The nuclei were stained with 4',6-diamidino-2-phenylindole (DAPI). Samples were mounted with a VECTASHIELD (Vector Laboratories).

Western blotting: Cells and tissue were lysed with lysis buffer (Cell signaling Technology, Danvers, MA) and scraped, and the supernatant was collected by centrifugation at 200 ×g for 10 min. Protein concentration was determined using BCA reagents (Thermo Scientific). The cell lysate was resolved with sodium dodecyl sulfate polyacrylamide gel electrophoresis (SDS–PAGE) and transferred to a nitrocellulose membrane. Membranes were incubated with the blocking solution (5% skim milk in Tris-buffered saline and Tween 20 [TBST]) for 1 h at RT and then incubated with primary Abs to α-SMA, N-cadherin, ZO-1, RPE65, E-cadherin, and GAPDH (Abcam) followed by anti-IgG horseradish peroxidase–conjugated secondary Ab. The blots were detected with enhanced chemiluminescence (GE healthcare, Chicaco, IL).

Statistical analysis: Data are presented as mean ± standard deviation of the mean (SD). P values of less than 0.05 were interpreted as statistically significant and denoted by * for $p<0.05$, ** for $p<0.01$, and *** for $p<0.001$.

RESULTS

SP blocks dispase-induced PVR-like conditions in vivo: Intravitreal injection of dispase is used to explore the development of PVR-like conditions in vivo. It has been suggested that dispase injection can disrupt the inner limiting membrane and penetrate the retina, impairing blood vessels. This can induce an inflammatory response, not only in the vitreous and retina but also in the anterior chamber [35,36], and cause fibrosis and retinal detachment. When the retina detaches, the RPE layer becomes dysfunctional, which leads to reduction of cell viability in the retina and degeneration [33,34,37]. To induce a PVR-like retinal condition, dispase was intravitreally injected, and SP was administered systemically. Histological change was monitored for 3 weeks to determine the effect of SP on the onset of PVR.

Histological analysis at 1 week post-dispase injection showed that the severe disrupted structure was rarely detected in the saline- and SP-treated groups, and the retina layer seemed to be primarily intact (Figure 1A). Analysis of the cellular density in the INL and the ONL showed that cell viability in each layer was slightly decreased by dispase injection, which was blocked by SP treatment (Figure 1B: INL, 70.8±6.00 nuclei in the normal group, 48.2±5.10 nuclei in the saline-treated group, and 60.7±2.00 nuclei in the SP-treated group, saline- versus SP-treated groups, $p<0.001$; Figure 1C: ONL, 24±3 nuclei in the normal group, 19.3±2.10 nuclei in the saline-treated group, and 22.5±1.50 nuclei in the SP-treated group, saline- versus SP-treated groups, $p<0.001$). CD31+ vasculature was detected in the saline-treated group, and the SP treatment slightly reduced the formation of vessels (Appendix 2). At 3 weeks post-dispase injection, a destroyed retinal structure with a blurred boundary between the INL and the ONL was observed in the saline-treated group, but the SP treatment markedly decreased the severity of the retina damage (Figure 1D). Quantitative analysis of the cell density in the ONL and the INL revealed that SP treatment obviously blocked cell loss from dispase-induced retinal damage (Figure 1E,F). Folding of the retina is an early phenomenon of PVR and gradually develops, followed by the formation of the fibrous membrane, which means a change in the retinal cell shape occurs. Figure 1D showed that the saline-treated

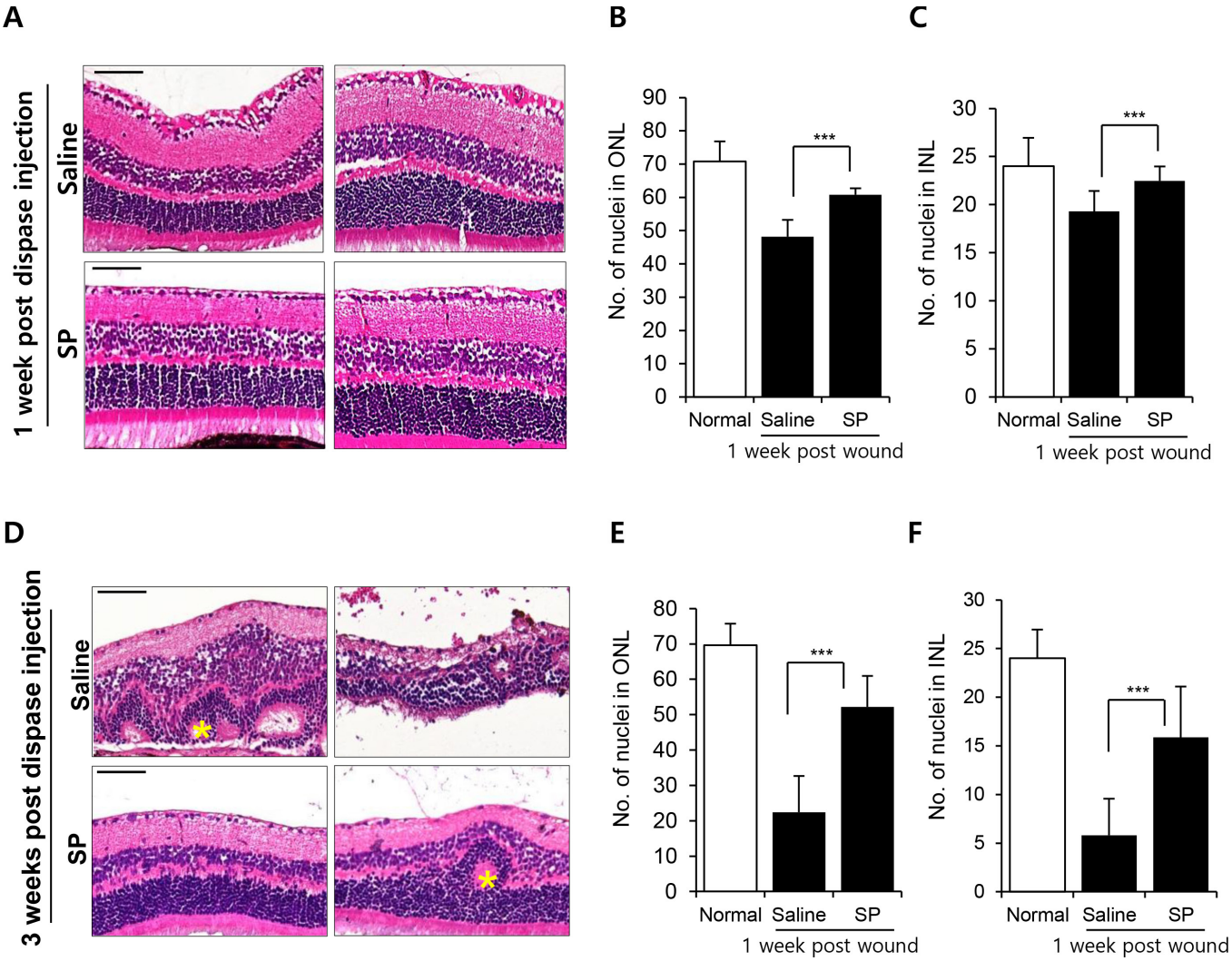

Figure 1. SP blocked dispase-induced retinal damage in vivo. Intravitreal injection of dispase was performed. One and three weeks later, the retinal structure was analyzed based on histology. **A**: Representative micrographs showing hematoxylin and eosin staining of retinal tissue in the saline- or substance P (SP)–treated groups at 1 week post-dispase injection. **B**,**C**: The mean number of nuclei in (**B**) the outer nuclear layer (ONL) and (**C**) the inner nuclear layer (INL) were measured. **D**: Hematoxylin and eosin staining of retinal tissue in the saline- or SP-treated groups at 3 weeks post-dispase injection. **E**,**F**: The mean number of nuclei in the ONL and the INL. Data are presented as mean ± the standard deviation (SD). Asterisk: rosette and folding structure. Scale bar: 50 µm. The mean measurement for six images in each tissue sample was calculated for each animal. *p<0.05; **p<0.01; ***p<0.001; n=8 mice per group.

group had complicated enfolding and rosette-shaped cellular invagination, whereas the INL and the ONL were more intact with less folding in the SP-treated group. These data suggest that SP can inhibit the development of dispase-induced injury, possibly by blocking retinal enfolding and preserving cell viability.

SP inhibits apoptosis and cellular transition by alleviating the inflammatory response due to retinal damage: Dispase-induced damage may lead to retinal inflammation, which eventually accelerates disease progression. Thus, inhibition of inflammatory response is anticipated to be the critical treatment for PVR. A previous study demonstrated that SP is capable of inducing transition of M1-type macrophages to the M2 type, with a reduction in TNF-α and an increase in IL-10 [25,27] and exerting an anti-inflammatory effect on a variety of diseases. To investigate whether systemically injected SP is able to suppress inflammation from retina damage or not, the change in serum cytokines was examined. As shown in Figure 2A, the dispase injection evoked the systemic inflammation. The TNF-α level in serum was elevated in the saline-treated group but was reduced in the SP-treated group. The level of IL-10 was similar in the normal and saline-treated groups

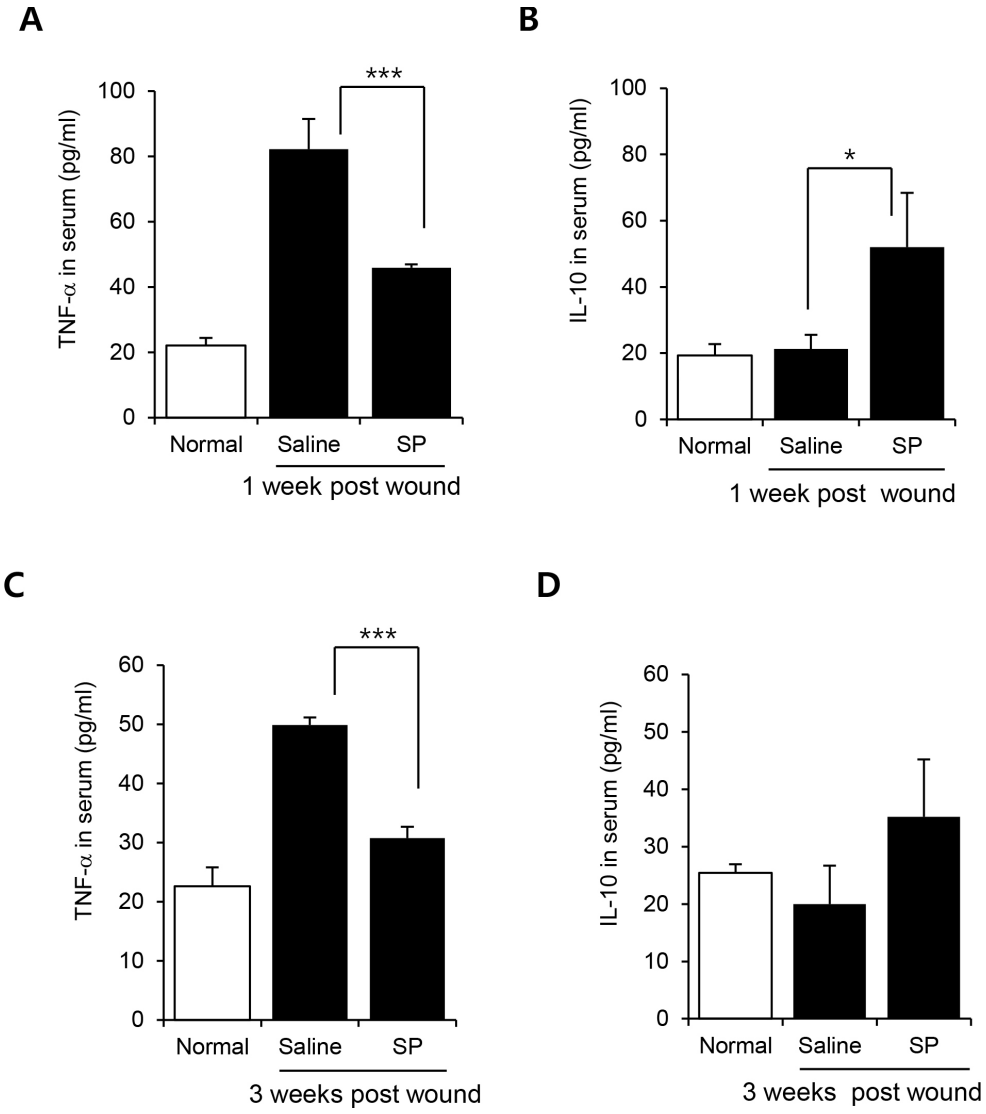

Figure 2. Retinal injury-induced inflammation is suppressed by SP. At 1 and 3 weeks post-dispase injection, serum was collected, and the cytokine profile was analyzed with enzyme-linked immunosorbent assay (ELISA). **A**,**B**: Tumor necrosis factor-alpha (TNF-α) and interleukin-10 (IL-10) in serum 1 week post-dispase injection. **C**,**D**: TNF-α and IL-10 in serum 3 weeks post-dispase injection. *p<0.05; ***p<0.001; n=8 mice per group.

but markedly increased in the SP-injected group (Figure 2B). This trend was sustained for 3 weeks post-dispase injection, although the difference among the experimental groups was reduced (Figure 2C,D). That is, SP could modulate inflammatory cytokine profiles in serum in the early stages after the dispase injection wound, which might be deeply associated with retinal protection.

Next, we examined whether SP-mediated retina protection is accompanied by reduction of inflammatory mediators at the impaired retina. Because SP affected systemic inflammation at 1 week post-dispase injection, local inflammation was also inferred to be mitigated by SP. As a representative proinflammatory cytokine, TNF-α was analyzed with immunohistochemical staining. The staining intensity of TNF-α was quantitatively analyzed. Figure 3A shows that TNF-α was strongly expressed through all layers of the retina in the saline-treated group, but the TNF-α level was decreased by the SP treatment (Figure 3A,B). The level of TNF-α was confirmed with western blotting (Figure 3G). TNF-α is the main promoter of neuroinflammation within the retina layer and causes cell apoptosis. As TNF-α secretion in the retina layer was reduced in the SP-treated group, it was surmised that SP could prevent TNF-α-induced cell death. To check this hypothesis, apoptotic cells were examined with immunohistochemical staining of cleaved caspase-3. In accordance with previous reports, the strong expression of TNF-α led to cellular apoptosis, but SP treatment decreased the number of apoptotic cells as 70% less than that of the saline-treated group (Figure 3C,D: 10.1±2.70% in the saline-treated group and 2.8±2.2% in the SP-treated group, saline- versus SP-treated groups, p<0.05). Western blotting for cleaved

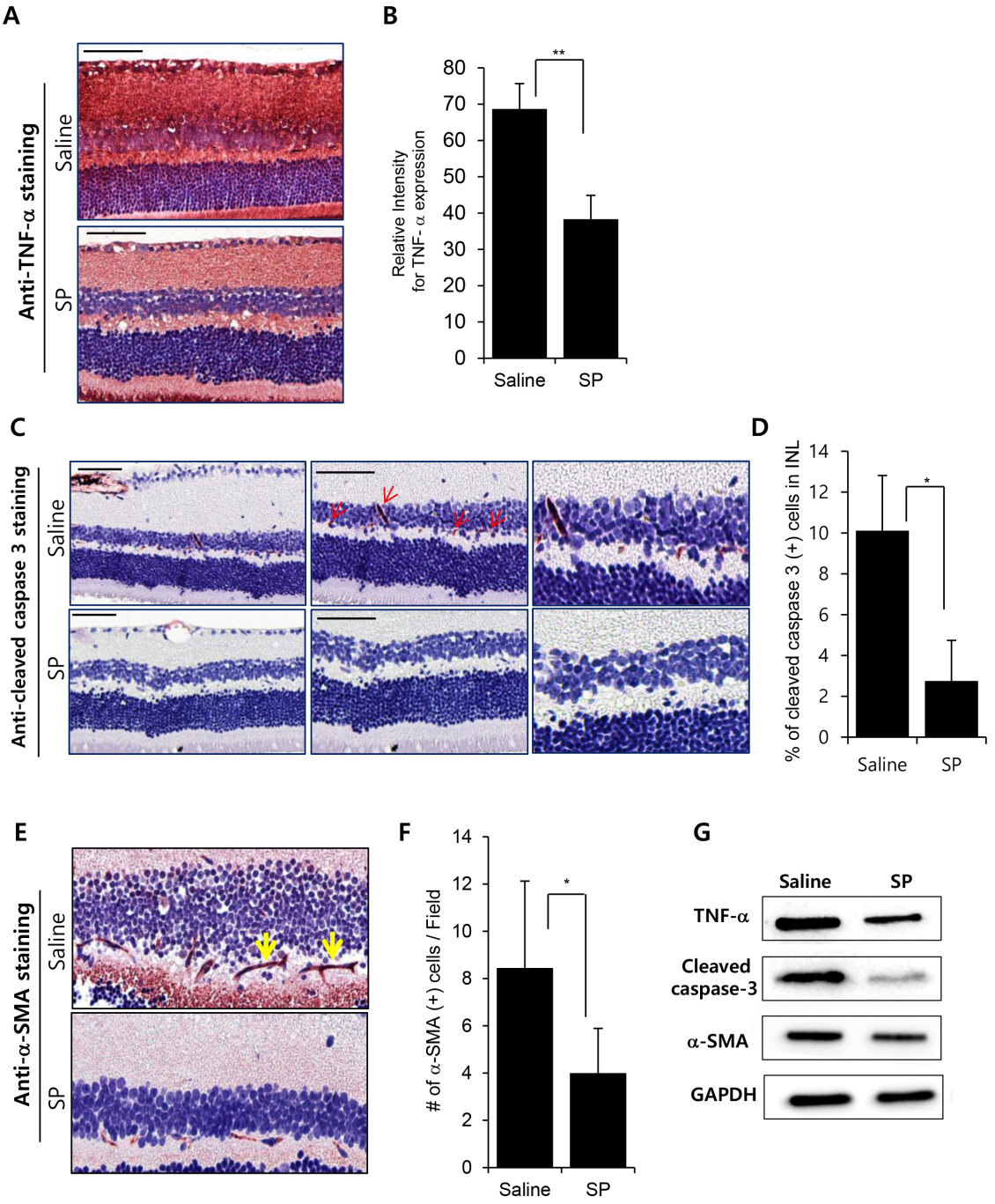

Figure 3. SP-induced suppression of local inflammation contributes to the inhibition of cellular apoptosis and α-SMA (+) cell infiltration at wound sites. **A**,**B**: Immunohistochemical staining for tumor necrosis factor-alpha (TNF-α) was performed, and the intensity of the stained area was measured using the ImageJ program. **C**,**D**: Analysis of the apoptotic cells in the retina was performed. To elucidate the apoptotic cells, cleaved caspase 3 (+) cells were counted in the inner nuclear layer (INL). Red arrow: cleaved caspase 3 (+) cells. **E**,**F**: Alpha smooth muscle actin (α-SMA) (+) fibroblastic cells migrated toward the INL were observed and quantitatively assessed. **G**: Level of TNF-α, cleaved caspase-3, and α-SMA were determined by western blotting. The mean measurement of the six images in each tissue sample was calculated in each animal. Data are presented as mean ± standard deviation (SD). Scale bar: 50 µm. *p<0.05; **p<0.01; n = 8 mice per group.

caspase-3 was conducted, demonstrating the reduction of the cleaved caspase 3 level by the SP treatment (Figure 3G).

PVR is characterized by EMT via an inflammatory signal including TNF-α. In the EMT process, cells lose epithelial characteristics, such as specialized cell-to-cell contact, and acquire migratory mesenchymal properties [5,38]. These processes are mediated by cytoskeletal reorganization as actin filaments. TNF-α is found to induce the EMT of the RPE, as well as cell apoptosis. Thus, the TNF-α-enriched environment post-retinal impairment by dispase was estimated to trigger the transdifferentiation of the RPE into mesenchymal cells. Diminished secretion of TNF-α by SP was likely to hardly cause the cellular transition of the RPE. To examine the existence of mesenchymal cells in the retina, the distribution of alpha smooth muscle actin (α-SMA) (+) fibroblastic cells was determined with immunohistochemical staining. Figure 3 shows α-SMA (+) fibroblastic cells migrating toward INL. α-SMA (+) fibroblastic cells were observed in the saline- and SP-treated groups, but the number was much higher in the saline-treated group than in the SP-treated group (Figure 3E,F: 8.45±3.70 cells in the saline-treated group and 4.0±1.9 cells in the SP-treated group, saline- versus SP-treated groups, $p<0.01$). Taken together, these data indicate that SP can reverse early inflammatory responses, which might contribute to the blockage of cell death and mesenchymal transition, ultimately leading to the inhibition of retinal detachment and the development of PVR.

SP blocks TNF-α-induced transdifferentiation of the RPE in vitro: Inhibition of TNF-α secretion by SP was presumed to be sufficient to prevent the onset of PVR in vivo. Retina degeneration was hindered by the anti-inflammatory effect of SP (Figure 3). In addition, based on studies of the role of SP in cell junctional molecule expression [30] and TNF-α-induced cellular change in epithelial cells [29], SP was expected to act on epithelial cells to reduce the susceptibility to the transition by TNF-α and preserve epithelial characteristics. After confirming the expression of NK-1R on the RPE (data not shown), the human RPE cell line ARPE-19 was treated with SP in the presence of TNF-α, and cellular characteristics were investigated (Figure 4A). Analysis of the cytoskeletal structure with F-actin staining showed that while the control exhibited cell-to-cell-contact-enriched actin microfilaments, the TNF-α-treated RPE possessed well-organized actin stress fibers throughout the cell body. However, cotreatment of SP inhibited TNF-α-induced cytoskeletal reorganization, resulting in an actin microfilament structure similar to that of the untreated control (Figure 4B). α-SMA and N-cadherin, markers specific to the mesenchymal cell type during EMT, were checked with immunofluorescence staining and western blotting (Figure 4C,D). As predicted, α-SMA was not detected in the untreated control, whereas TNF-α exposure for 48 h induced strong expression of α-SMA in the RPE. SP treatment suppressed TNF-α-induced expression of α-SMA. Consistent with the expression pattern of α-SMA, the expression level of N-cadherin slightly increased post-TNF-α treatment but was reduced with SP treatment. The EMT of the RPE by TNF-α was also accompanied by the loss of RPE characteristics for RPE65, ZO-1, and E-cadherin. This phenomenon was thoroughly reversed by SP (Figure 4E). Collectively, these results demonstrate that SP can directly prevent epithelial to mesenchymal changes in cellular characteristics related to TNF-α; the effect is also linked to the therapeutic effects of SP on PVR.

DISCUSSION

RRD induces a breakdown in the BRB, triggering migration and proliferation of diverse cells, including the RPE, fibrous astrocytes, fibroblasts, myofibroblasts, and macrophages, leading to inflammation and the onset of PVR. As current strategies for RRD and PVR, surgery pneumatic retinopexy, scleral buckling, and pars plana vitrectomy have been attempted to establish choroid-retinal adhesion around retinal damage. Chemical inhibition of cell proliferation and membrane contraction are also employed. However, in spite of multiple trials, recurrent detachment remains a serious issue, and effective treatment strategies continue to be elusive.

In this study, we investigated the role of SP in a dispase-induced retinal impaired murine model. Intravitreal injection of dispase provoked the occurrence of severe destruction with retinal enfolding within 3 weeks. However, early treatment of SP blocked dispase-induced retinal damage and maintained a more intact retinal structure compared to saline-treated animals. Although the difference in retinal structure between the saline- and SP-treated groups was clarified at 3 weeks post dispase-injection, this difference was thought to be attributed to SP-mediated cellular and physiologic changes occurring early post-SP injection. Analysis for serum cytokine indicated the cytokine profile was reversed by SP treatment 1 week post-dispase injection. The retina structure seemed to be stable at 1 week, but inflammation was certainly initiated, as shown in the strong expression of TNF-α in the retinal tissue. This inflammatory environment caused apoptosis and the appearance of fibroblastic cells, which might bring out severe retina damage at 3 weeks post dispase-injection. Meanwhile, the early blockage of local inflammatory signs by SP preserved cellular viability against apoptosis and decreased the infiltration of α-SMA (+) fibroblastic cells, rendering the retinal structure more intact. The

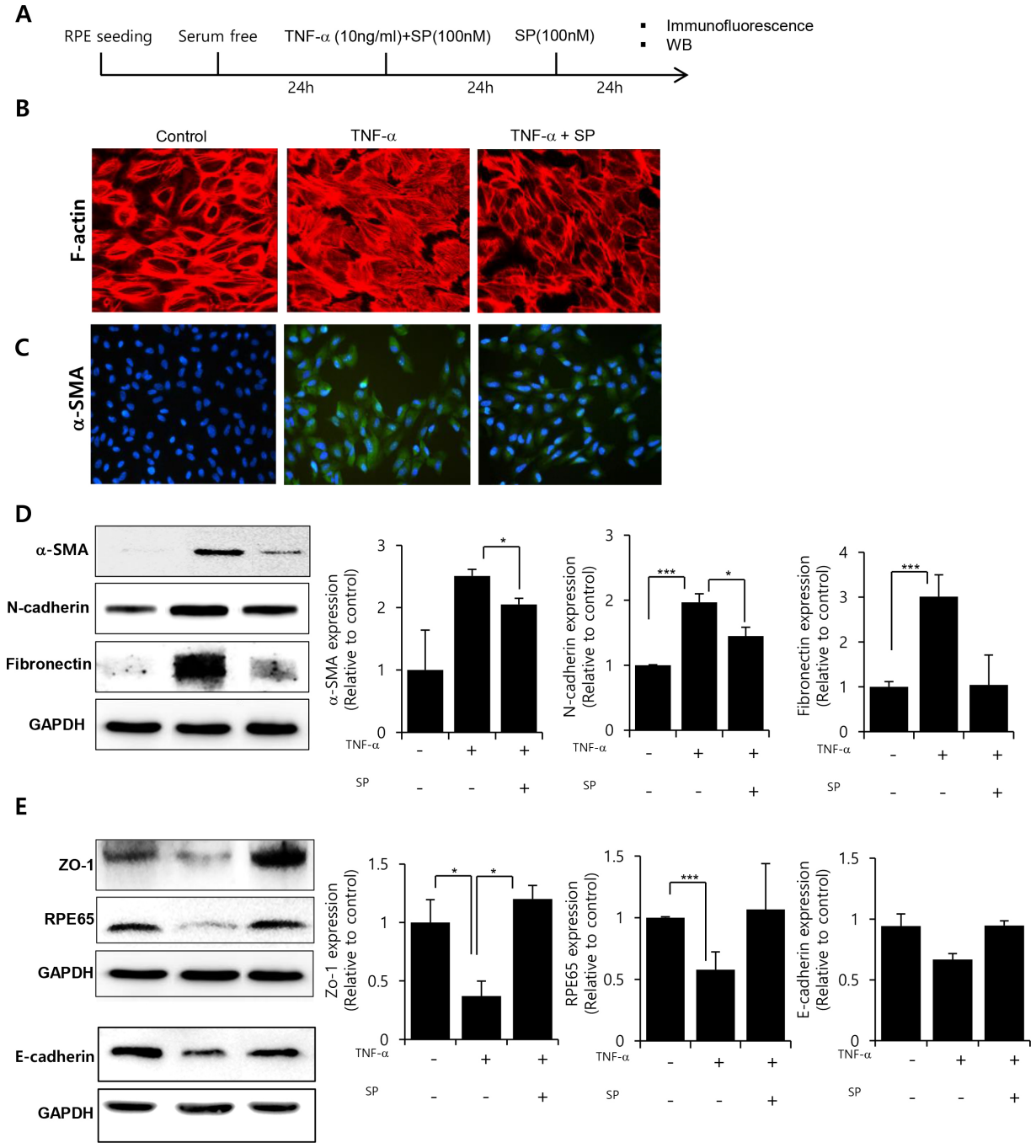

Figure 4. SP blocks TNF-α-induced transdifferentiation of RPE in vitro. **A**: Experimental schedule for tumor necrosis factor-alpha (TNF-α) and substance P (SP) treatment in ARPE-19 cells in vitro. After serum starvation for 24 h, TNF-α (10 ng/ml) was added to the ARPE-19 cells with SP (100 nM), and 24 h later, the SP treatment was repeated. **B,C**: Cytoskeleton rearrangement in the RPE was observed with immunofluorescence staining for F-actin and alpha smooth muscle actin (α-SMA). Scale bar: 100 µm. **D**: Analysis of the mesenchymal characteristics of α-SMA and N-cadherin was performed with western blotting and quantified relatively. **E**: RPE65, ZO-1 and E-cadherin, RPE characteristics were examined with western blotting. All experiments were performed in triplicate. *p<0.05; ***p<0.001.

early modulation of inflammation by SP is likely to reduce the potential for PVR development in vivo.

The reduction of inflammatory mediator by SP is critical to block the progression of retinal degeneration. In addition to this effect, this study demonstrated that SP is capable of inhibiting TNF-α-induced cellular transition in the RPE [39]. TNF-α provoked morphological change in the RPE, showing a lack of intercellular junctions and a gain of spindle cell morphology. Molecular analysis revealed that the TNF-α-treated RPE had increased expression of α-SMA and N-cadherin with the loss of ZO-1, RPE65, and E-cadherin. In contrast, SP was able to halt the cellular transition of the RPE due to TNF-α, conserving the expression level of ZO-1, RPE65, and E-cadherin with little expression of α-SMA. That is, SP could block the EMT of the RPE due to TNF-α.

In summary, SP treatment can provide anti-inflammatory effects by modulating cytokine profiles locally and systemically and can protect the retinal structure against PVR-like retinal damage. SP is also able to inhibit EMT of RPE by interfering with susceptibility to TNF-α. These novel functions of SP might lead to the prevention of PVR progression. Although the therapeutic effects of SP have been reported in diverse diseases, this is the first study to establish that the anti-inflammatory effects of SP through modulation of TNF-α can inhibit retinal damage in PVR. A safety study of SP revealed that long-term SP administration did not result in in vivo toxicity [40]. In addition, the different doses of SP did not exert a toxic effect on the RPE in vitro (Appendix 3).

Finally, this study provides the possibility to develop SP as a new drug for inflammation-related retinal diseases, including PVR. Further detailed study of the effect of SP on the EMT using the primary RPE and on diverse inflammatory disease will be undertaken to investigate the mechanism of action of SP in detail.

APPENDIX 1. ANLYSIS FOR STR FOR ARPE-19.

To access the data, click or select the words "Appendix 1"

APPENDIX 2. EVALUATION OF VASCULARIZATION IN THE INJURED RETINA

To access the data, click or select the words "Appendix 2"

APPENDIX 3. THE EFFECT OF SP ON RPE VIABILITY

To access the data, click or select the words "Appendix 3"

ACKNOWLEDGMENTS

This study was supported by a Korean Health Technology R&D Project grant (HI13C1479) from the Ministry of Health and Welfare (Sejong, Republic of Korea). Hyun Sook Hong, (hshong@khu.ac.kr) and Seung-Young Yu (syyu@khu.ac.kr) are co-corresponding authors for this paper.

REFERENCES

1. Cowley M, Conway BP, Campochiaro PA, Kaiser D, Gaskin H. Clinical risk factors for proliferative vitreoretinopathy. Arch Ophthalmol 1989; 107:1147-51. [PMID: 2757544].
2. Pastor JC, de la Rua ER, Martin F. Proliferative vitreoretinopathy: Risk factors and pathobiology. Prog Retin Eye Res 2002; 21:127-44. [PMID: 11906814].
3. Ryan SJ. The pathophysiology of proliferative vitreoretinopathy and its management. Am J Ophthalmol 1985; 100:188-93. [PMID: 4014372].
4. Lee J, Ko M, Joo CK. Rho Plays a Key Role in TGF-b1-Induced Cytoskeletal Rearrangement in Human Retinal Pigment Epithelium. J Cell Physiol 2008; 216:520-6. [PMID: 18314880].
5. Bochaton-Piallat ML, Kapetanios AD, Donati G, Redard M, Gabbiabi G, Pournaras CJ. TGF-beta1, TGF-beta receptor II and ED-A fibronectin expression in myofibroblast of vitreoretinopathy. Invest Ophthalmol Vis Sci 2000; 41:2336-42. [PMID: 10892881].
6. Sheridan CM, Occleston NL, Hiscott P, Kon CH, Khaw PT, Grierson I. Matrix metalloproteinases: A role in the contraction of vitreo-retinal scar tissue. Am J Pathol 2001; 159:1555-66. [PMID: 11583981].
7. Grisanti S, Guidry C. Transdifferentiation of retinal pigment epithelial cells from epithelial to mesenchymal phenotype. Invest Ophthalmol Vis Sci 1995; 36:391-405. [PMID: 7531185].
8. Connor TB, Roberts AB, Sporn MB, Danielpour D, Dart LL, Michels RG, de Bustros S, Enger C, Kato H, Lansing M. Correlation of fibrosis and transforming growth factor-beta type 2 levels in the eye. J Clin Invest 1989; 83:1661-6. .
9. Gaudric A, Glacet Bernard A, Clement G, Falquerho L, Barritault D, Coscas G. Transforming growth factor beta in the vitreous of patients with epiretinal proliferation. Ophthalmologie 1990; 4:51-2. [PMID: 2250941].
10. Limb GA, Little BC, Meager A, Ogilvie JA, Wolstencroft RA, Franks WA, Chignell AH, Dumonde DC. Cytokines in proliferative vitreoretinopathy. Eye (Lond) 1991; 5:686-93. [PMID: 1800167].
11. Oberhammer F, Wilson JW, Dive C, Morris ID, Hickman JA, Wakeling AE, Walker PR, Sikorska M. Apoptotic death in epithelial cells: cleavage of DNA to 300 and}or 50 kb fragments prior to or in the absence of internucleosomal fragmentation. EMBO J 1993; 12:3679-3664. [PMID: 8253089].

12. Weller M, Constam DB, Malipiero U, Fontana A. Transforming growth factor-b2 induces apoptosis of murine T cell clones without downregulating bcl-2 mRNA expression. Eur J Immunol 1994; 24:1293-300. [PMID: 8206089].

13. Esser P, Heimann K, Bartz-schmidt KU, Fontana A, Schraermeyer U, Thumann G, Weller M. Apoptosis in Proliferative Vitreoretinal Disorders: Possible Involvement of TGF-b-induced RPE cell Apoptosis. Exp Eye Res 1997; 65:365-78. [PMID: 9299173].

14. Grisanti S, Guidry C. Transdifferentiation of retinal pigment epithelial cells from epithelial to mesenchymal phenotype. Invest Ophthalmol Vis Sci 1995; 36:391-405. [PMID: 7531185].

15. Casaroli-Marano RP, Pagan R, Vilaró S. Epithelial-mesenchymal transition in proliferative vitroretinopathy: intermediate filament protein expression in retinal pigment epithelial cells. Invest Ophthalmol Vis Sci 1999; 40:2062-72. [PMID: 10440262].

16. Li H, Li M, Xu D, Zhao C, Liu G, Wang F. Overexpression of Snail in retinal pigment epithelial triggered epithelial–mesenchymal transition. Biochem Biophys Res Commun 2014; 446:347-51. [PMID: 24607896].

17. Takahashi E, Nagano O, Ishimoto T, Yae T, Suzuki Y, Shinoda T, Nakamura S, Niwa S, Ikeda S, Koga H, Tanihara H, Saya H. Tumor Necrosis Factor- Regulates Transforming Growth Factor–dependent Epithelial-Mesenchymal Transition by Promoting Hyaluronan-CD44-Moesin Interaction. J Biol Chem 2010; 285:4060-73. [PMID: 19965872].

18. Reitamo S, Remitz A, Tamai K, Uitto J. Interleukin-10 modulates type I collagen and matrix metalloproteinase gene expression in cultured human skin fibroblasts. J Clin Invest 1994; 94:2489-92. [PMID: 7989607].

19. Carrington L, McLeod D, Boulton M. IL-10 and antibodies to TGF-beta2 and PDGF inhibit RPE-mediated retinal contraction. Invest Ophthalmol Vis Sci 2000; 41:1210-6. [PMID: 10752962].

20. Rameshwar P, Zhu G, Donnelly RJ, Qian J, Ge H, Goldstein KR, Denny TN, Gascón P. The dynamics of bone marrow stromal cells in the proliferation of multipotent hematopoietic progenitors by substance P: an understanding of the effects of neurotransmitter on the differentiating hematopoietic stem cell. J Neuroimmunol 2001; 121:22-31. [PMID: 11730936].

21. Nakamura M, Kawahara M, Morishige N, Chikama T, Nakata K, Nishida T. Promotion of corneal epithelial wound healing in diabetic rats by the combination of a substance P–derived peptide (FGLM-NH2) and insulin-like growth factor-1 Diabetologia 2003; 46:839-42. [PMID: 12764579].

22. Hong HS, Lee J, Lee E, Kwon YS, Lee E, Ahn W, Jiang MH, Kim JC, Son Y. A new role of substance P as an injury-inducible messenger for mobilization of CD29+ stromal-like cells. Nat Med 2009; 15:425-35. .

23. An YS, Lee E, Kang MH, Hong HS, Kim MR, Jang WS, Son Y, Yi JY. Substance P stimulates the recovery of bone marrow after the irradiation. J Cell Physiol 2011; 226:1204-13. .

24. Kang MH, Kim DY, Yi JY, Son Y. Substance-P accelerates intestinal tissue regeneration after gamma irradiation-induced damage. Wound Repair Regen 2009; 17:216-23. [PMID: 19320890].

25. Jiang MH, Chung E, Chi GF, Ahn W, Lim JE, Hong HS, Kim DW, Choi H, Kim J, Son Y. Substance P induces M2-type macrophages after spinal cord injury. Neuroreport 2012; 23:786-92. .

26. Delgado AV, McManus AT, Chambers JP. Exogenous administration of Substance P enhances wound healing in a novel skin-injury model. Exp Biol Med 2005; 230:271-80. [PMID: 15792949].

27. Hong HS, Son Y. Substance P ameliorates collagen II-induced arthritis in mice via suppression of the inflammatory response. Biochem Biophys Res Commun 2014; 453:179-84. [PMID: 25264193].

28. Hong HS, Kim S, Nam S, Um J, Kim YH, Son Y. Effect of substance P on recovery from laser-induced retinal degeneration. Wound Repair Regen 2015; 23:268-77. [PMID: 25682893].

29. Backman LJ, Eriksson DE, Danielson P. Substance P reduces TNF-α-induced apoptosis in human tenocytes through NK-1 receptor stimulation. Br J Sports Med 2014; 48:1414-20. [PMID: 23996004].

30. Ko JA, Yanai R, Nishida T. Up-regulation of ZO-1 expression and barrier function in cultured human corneal epithelial cells by substance P. FEBS Lett 2009; 583:2148-53. [PMID: 19446555].

31. Cantó Soler MV, Gallo JE, Dodds RA, Suburo AM. A mouse model of proliferative vitreoretinopathy induced by dispase. Exp Eye Res 2002; 75:491-504. [PMID: 12457862].

32. Iribarne M, Ogawa L, Torbidoni V, Dodds CM, Dodds RA, Suburo AM. Blockade of Endothelinergic Receptors Prevents Development of Proliferative Vitreoretinopathy in Mice. Am J Pathol 2008; 172:1030-42. [PMID: 18310504].

33. Isiksoy S, Basmak H, Kasapoglu Dundar E, Ozer A. Expression of proteins associated with cell-matrix adhesion in proliferative vitreoretinopathy designed by Dispase mode. Eur J Ophthalmol 2007; 17:89-103. [PMID: 17294388].

34. Frenzel EM, Neely KA, Walsh AW, Cameron JD, Gregerson DS. A new model of proliferative vitreoretinopathy. Invest Ophthalmol Vis Sci 1998; 39:2157-64. [PMID: 9761295].

35. Jorge R, Oyamaguchi EK, Cardillo JA, Gobbi A, Laicine EM, Haddad A. Intravitreal injection of dispase causes retinal hemorrhages in rabbit and human eyes Curr Eye Res 2003; 26:107-12. [PMID: 12815529].

36. Pastor JC, de la Rua ER, Martin F. Proliferative vitreoretinopathy: risk factors and pathobiology. Prog Retin Eye Res 2002; 21:127-44. [PMID: 11906814].

37. Sheridan CM, Occleston NL, Hiscott P, Kon CH, Khaw PT, Grierson I. Matrix metalloproteinases: a role in the contraction of vitreo-retinal scar tissue. Am J Pathol 2001; 159:1555-66. [PMID: 11583981].

38. Choi K, Lee K, Ryu SW, Im M, Kook KH, Choi C. Pirfenidone inhibits transforming growth factor-β1-induced fibrogenesis by blocking nuclear translocation of Smads in human retinal pigment epithelial cell line ARPE-19. Mol Vis 2012; 18:1010-20. [PMID: 22550395].

39. Li H, Wang H, Wang F, Gu Q, Xu X. Snail Involves in the Transforming Growth Factor b1-Mediated Epithelial-Mesenchymal Transition of Retinal Pigment Epithelial Cells. PLoS One 2011; 6:e23322-[PMID: 21853110].

40. Hong HS, Lim SV, Son Y. Evaluation of substance-P toxicity with single dose and repeated dose. Mol Cell Toxicol 2015; 11:201-11. .

Articles are provided courtesy of Emory University and the Zhongshan Ophthalmic Center, Sun Yat-sen University, P.R. China. The print version of this article was created on 13 December 2017. This reflects all typographical corrections and errata to the article through that date. Details of any changes may be found in the online version of the article.